Letter

Wissam Farhat[a], Arne Stamm[a], Maxime Robert-Monpate[b], Antonino Biundo and Per-Olof Syrén*

Biocatalysis for terpene-based polymers

https://doi.org/10.1515/znc-2018-0199
Received November 30, 2018; revised January 23, 2019; accepted January 24, 2019

Abstract: Accelerated generation of bio-based materials is vital to replace current synthetic polymers obtained from petroleum with more sustainable options. However, many building blocks available from renewable resources mainly contain unreactive carbon-carbon bonds, which obstructs their efficient polymerization. Herein, we highlight the potential of applying biocatalysis to afford tailored functionalization of the inert carbocyclic core of multicyclic terpenes toward advanced materials. As a showcase, we unlock the inherent monomer reactivity of norcamphor, a bicyclic ketone used as a monoterpene model system in this study, to afford polyesters with unprecedented backbones. The efficiencies of the chemical and enzymatic Baeyer–Villiger transformation in generating key lactone intermediates are compared. The concepts discussed herein are widely applicable for the valorization of terpenes and other cyclic building blocks using chemoenzymatic strategies.

Keywords: biocatalysis; biopolymers; oxidoreductases; polyesters; terpenes.

[a]**Wissam Farhat and Arne Stamm:** These authors contributed equally to this work.
[b]**Present address:** Ecole supérieure de chimie organique et minérale, 1 Allée du Réseau Jean Marie Buckmaster, 60200 Compiègne, France
***Corresponding author: Per-Olof Syrén,** Department of Fibre and Polymer Technology, School of Engineering Sciences in Chemistry, Biotechnology and Health, KTH Royal Institute of Technology, Teknikringen 56-58, 100 44 Stockholm, Sweden; Science for Life Laboratory, School of Engineering Sciences in Chemistry, Biotechnology and Health, KTH Royal Institute of Technology, Tomtebodavägen 23, Box 1031, 171 21 Solna, Stockholm, Sweden; and Wallenberg Wood Science Center, Teknikringen 56-58, SE-100 44 Stockholm, Sweden, E-mail: per-olof.syren@biotech.kth.se. https://orcid.org/0000-0002-4066-2776
Wissam Farhat, **Arne Stamm**, **Maxime Robert-Monpate and Antonino Biundo:** Department of Fibre and Polymer Technology, School of Engineering Sciences in Chemistry, Biotechnology and Health, KTH Royal Institute of Technology, Teknikringen 56-58, 100 44 Stockholm, Sweden; and Science for Life Laboratory, School of Engineering Sciences in Chemistry, Biotechnology and Health, KTH Royal Institute of Technology, Tomtebodavägen 23, Box 1031, 171 21 Solna, Stockholm, Sweden

1 Introduction

With tens of thousands of different molecular architectures currently known, terpenes constitute one of the most diversified families of natural products [1]. Terpenes display potent biological activities [2] and have important application areas as fine chemicals, flavors, fragrances, and as anticancer, antibacterial, and antiviral agents [1, 3]. As the stereospecific generation of poly(hetero)cyclic terpenoids in high yields by synthetic chemistry can constitute a formidable challenge [4, 5], biosynthesis of terpene-based synthons is a contemporary research area [6]. One option is to generate desired terpene-derived products through metabolic engineering efforts starting from sugars [7], or even CO_2 as demonstrated recently [8]. In addition, as terpenes are of fundamental importance to all life forms [9], these renewable metabolites are also readily available for biocatalytic valorization from natural sources, either by in vitro methods or by using whole cell catalysts. In fact, approximately 0.5×10^9 tons of biotic carbons, originating mainly from monoterpenes, are released into the atmosphere each year [10, 11]. This very large quantity is smaller than the total amount of polysaccharides generated (~150×10^9 tons/year [12]). Nevertheless, the unique, multicyclic facet of terpenoids makes this family of natural products highly interesting as chiral building blocks for manufacturing of advanced biochemicals and biomaterials. Herein, we highlight the potential of biocatalytic upgrading of terpenes and terpene analogues toward novel bio-based polymers. The possibility of biocatalytic expansion of terpene reaction space is discussed, with an emphasis on oxy-functionalization. We demonstrate the feasibility of using this concept by valorization of norcamphor, representing a bicyclic monoterpene-model substrate herein. Chemical polymerization

of the targeted norcamphor-based lactone successfully afforded an unprecedented polyester harboring a cyclopentane ring protruding from its backbone. Our results stress the untapped potential of terpene-derived building blocks as a platform for the generation of biochemicals and biopolymers [12, 13].

Elongated polyisoprenes are formed by the assembly of the universal C_5 terpene precursors isopentenyl pyrophosphate (IPP, **4**, Scheme S1, Supporting information) and dimethylallyl pyrophosphate (DMAPP, **5**, Scheme S1), catalyzed by prenyl transferase (PT) enzymes (see the Supporting information for details on fundamental terpene biosynthesis). Electrophilic polycyclization cascades of basal linear polyisoprenoids catalyzed by terpene cyclase (TC) enzymes (also referred to as terpene synthases) are key to generate a myriad of terpene-based skeletons (Figure 1, top right). TCs orchestrate the remarkable concerted, carbocationic cyclization cascade of the substrate that is already chaperoned in a productive precyclic conformation in the enzyme active site. Propagation of the highly reactive carbocation throughout the cyclization event drives stereospecific *C-C* bond formation and ring formation/expansion processes. Methyl and hydrogen transfers, possibly assisted by tunneling [15], contribute in generating product diversity. Termination occurs by deprotonation by a properly positioned base, or by water addition that leads to hydroxylated products. The work herein focuses on the potential of biocatalytic decoration of terpenes into added-value monomers amenable for polymerization (Figure 1). Four complementary strategies to achieve the challenging transformation into synthons with functional handles toward novel biomaterials are highlighted in Figure 1.

In principle, novel terpene-based biopolymers via biocatalysis could be afforded by capitalizing on (1) enzyme-catalyzed diversification of the linear substrate (Figure 1, top left box); (2) biocatalytic cyclization by TCs (Figure 1, top right box); (3) product functionalization (Figure 1, bottom right box); and finally (4) polymer synthesis. These strategies are briefly discussed below.

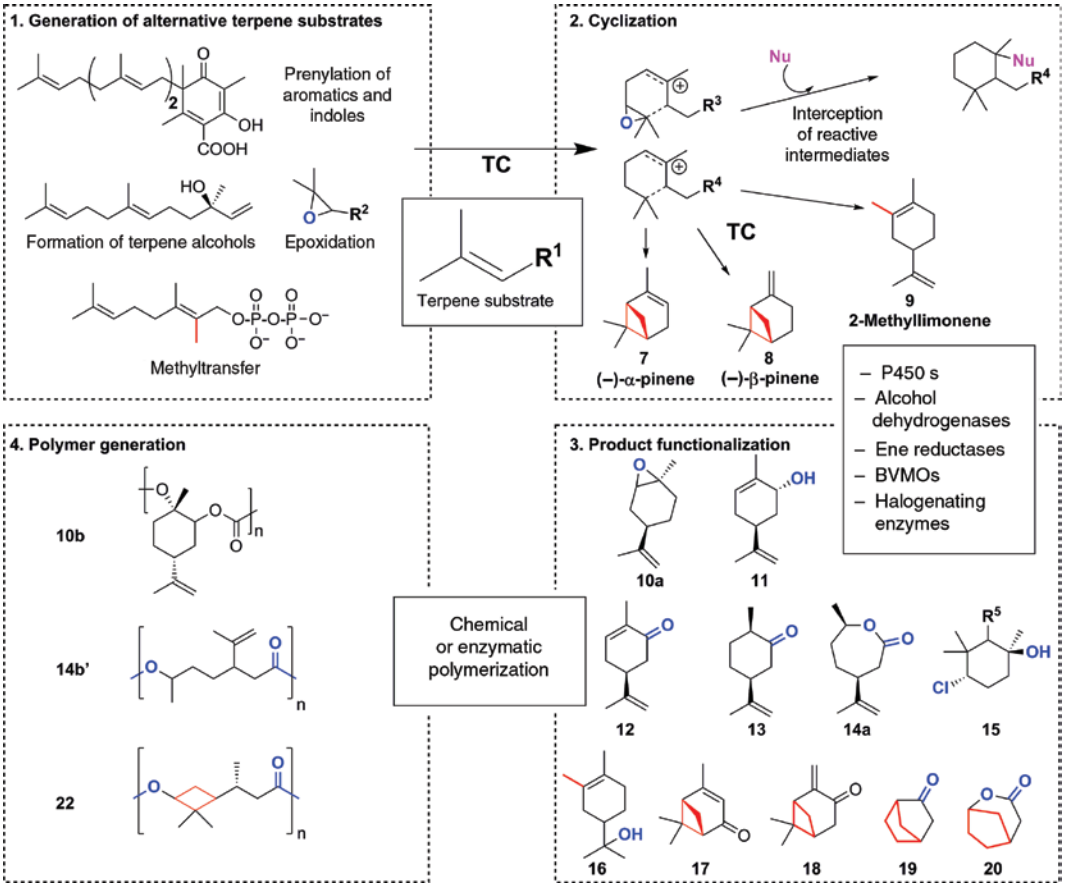

Figure 1: Biocatalytic strategies toward novel terpene-based polymers. For clarity, cofactors are omitted and only parts of the napyradiomycin [14] structure is shown as **15**. TC, terpene cyclase; BVMOs, Baeyer–Villiger monooxygenases; Nu, nucleophile. Polar functional groups are in blue and alkyl/cyclobutane is in red.

1.1 Extended substrate space

Prenylation of phenyls and indoles by aromatic PTs [16, 17] constitutes a highly interesting avenue to add terpene-based handles by biocatalysis. This is exemplified here by the biocatalytic addition of farnesyl pyrophosphate (FPP) to 3,5-dimethylorsellinic acid catalyzed by Trt2 from *Aspergillus fumigatus* [18], an aromatic PT. This transformation is formally an aromatic addition; one that is dependent on enzyme-catalyzed ionization of the pyrophosphate group of FPP. Aromatic PTs can display a different fold and active site architecture compared with that of the isoprenoid coupling enzymes shown in Scheme S1B.

Transfer of isoprene units is instrumental in assembling linear terpenes with other metabolites, such as indoles [19, 20]: a process of importance for bioactivity of some antibiotics [21]. Thus, Friedel–Crafts-like aromatic substitutions are known in biology. Promiscuous [20, 22] aromatic PTs are of particular biocatalytic interest toward the generation of fine chemical synthons and complex alkaloids [18, 22].

Generation of terpene-based alcohols can be imposed by carbocationic mechanisms of terpene synthases. Specifically, breakage of the labile allylic carbon-oxygen bond mediates the release of pyrophosphate, which is followed by water addition. This biotransformation is shown for *trans*,*trans*-nerolidol, which can be generated from FPP by sesquiterpene synthases [23].

Epoxidation of the terminal isoprene group by monooxygenases is instrumental for steroid biosynthesis. This biocatalytic process also reduces the activation barrier for subsequent cyclization steps, as protonation of an oxirane is facilitated compared with that of a terminal isoprene group.

Synthesis of alternative linear polyisoprenes through methylation of their backbone can remarkably bypass the well-known "isoprene rule" [24]. The biosynthesis of methyl-GPP (shown with methyl group in red), is founded on *S*-adenosylmethionine (SAM)-dependent methylation of **6**, catalyzed by geranyl diphosphate methyltransferase [25].

1.2 Cyclization

Cyclizations of (functionalized) linear terpenoids by TCs significantly expand terpene diversity. Cyclization of prenylated terpenes, obtained from strategy 1 above, is key to incorporate aromatic rings into multicyclic natural products, which tailors their bioactivity [18]. We and others have demonstrated the high potential of using class II TCs to generate polyheterocyclic building blocks through cyclization of terpene-based alcohols [26–28]. Epoxidized linear terpenes significantly expand reaction space by adding an additional functional handle (i.e. hydroxyl group) in generated cyclic product, which is of basal importance in plant biology and cell signaling [4]. Recently, metabolic engineering and promiscuous TCs were used to generate unprecedented cyclic C_{11} terpenes from methyl-GPP, exemplified here for 2-methyllimonene **9** [29]. The exciting possibility of interception of highly reactive carbocations generated during TC catalysis, by additional nucleophiles beyond water, have been demonstrated (corresponding to Nu = R-OH in Figure 1, top right) [30].

1.3 Product functionalization

Oxidation is one fundamental process to unlock the reactivity of cyclic building blocks for their controlled polymerization, e.g. via diols [31] and keto-groups shown for pinocarvone **18** [32]. Starting from cyclic building blocks generated by TCs above, and exemplified here by (−)-α-pinene (**7**), (−)-β-pinene (**8**), and 2-methyllimonene (**9**, Figure 1), P450 monooxygenases constitute potent biocatalysts to achieve oxidation of the carbocyclic ring(s) [33]. P450 monooxygenases are known to install oxirane groups (exemplified by limonene epoxide **10a**), alcohols (represented by (1*R*,5*S*)-carveol **11**) and even keto-groups (represented here by unsaturated carvone **12** and (−)-verbenone **17**) [34, 35]. Optionally, the emerging family of peroxygenases, which rely on hydrogen peroxide to generate the oxoferryl-heme intermediate, are known to afford the generation of terpene-based alcohols and epoxides [36, 37]. Alcohol dehydrogenases can readily generate keto-functionalized terpenes [38, 39] (e.g. **12** and **17**) from corresponding alcohols. Ene reductases [40] can afford subsequent reduction of the α,β-double bond in **12** to generate saturated carvone **13** [41]. Recently discovered [42] ene-reductases from natural product biosynthesis are expected to significantly advance the toolbox of terpene functionalization. Further oxidation of ketones into terpene-derived lactones by Baeyer–Villiger monooxygenases [43, 44] (BVMOs) is exemplified here for carvolactone **14a** generated from **13** [45].

With respect to product diversity, prenylation of non-terpene-derived motifs in meroterpenoids is abundant in nature [46]. Halogenation by vanadium haloperoxidases [47] generate cyclic and halogenated (mero)terpenoids [48], shown here for the napyradiomycin family of natural products (**15**). Recently, non-heme-dependent

iron dioxygenases have been in the spotlight for the generation of terpene-based diols (not shown) [49].

1.4 Polymerization

For linear terpenes, bio-based polyisoprene can be generated by pyrophosphate release from **4** catalyzed by isoprene synthase [23], followed by radical polymerization. Polymerization of decorated, multicyclic terpenoids, in particular obtained through enzymatic oxidation [37], constitutes a highly interesting strategy to generate bio-based materials with tailored backbone functionalization. This is shown here for limonene polycarbonate **10b**, which can be manufactured from *trans* limonene oxide **10a** [50]. We strongly believe that the introduction of the lactone functional group to cyclic building blocks will enable the design of new polymers. Recently, Messiha et al. investigated a semisynthetic approach using biocatalysis with renewable feedstocks as a venue to generate lactone monomers [51]. These monomers were polymerized using a mild metal-organic catalyst to result in the formation of previously unreported polymers [51]. For instance, carvone-lactone **14a** could generate polyesters with pendant alkyl chains as shown here for the previously published biopolymer **14b'**[52] (analogous polyesters can be assembled from (−)-menthide [53]). Another example of the valorization of renewable resource-derived monomers is the polymerization of a lactone derived from verbenone **17** into the biopolymer **22**, as recently demonstrated by us [54]. Poly(lactones) can be prepared by ring-opening polymerization (ROP) processes. ROP is a form of chain-growth polymerization in which the terminal end of the growing polymer will behave as a reactive moiety, enabling the addition of a cyclic monomer into the polymeric chain by ring opening. Three main mechanisms of ROP (anionic, cationic, and coordination-insertion) have been proposed based on the type of initiator/catalyst used [55, 56].

Anionic ring-opening polymerization (AROP) involves the addition of a small amount of a nucleophilic agent to attack the carbonyl carbon of the cyclic monomer and initiate its polymerization (Scheme 1A). This method can be efficiently controlled to produce high molecular weight polyesters. In contrast, cationic ring-opening polymerization (CROP) is a process that can be initiated by the addition of a trace amount of an electrophile to the cyclic monomer. In CROP, a positively charged intermediate will be formed and subsequently attacked by a cyclic monomer (Scheme 1B). In fact, not all cyclic esters undergo CROP. CROP depends on the ring size, to be more

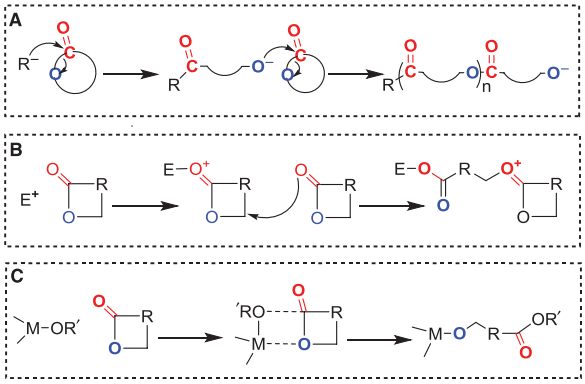

Scheme 1: Illustration of chain-growth in ROP processes. (A) Anionic, (B) cationic, and (C) coordination-insertion ROP. Reproduced from Stridsberg et al.

precise, on the ring strain. For instance, cyclic monomers with 4-, 6-, and 7-membered rings polymerize readily via CROP, unlike cyclic esters with smaller membered rings (or without ring strain); they will not be polymerized by CROP. On the other hand, coordination-insertion ring-opening polymerization (C-IROP) involve the coordination of the monomer to an active intermediate and then its insertion into the metal-oxygen bond by electron rearrangement (Scheme 1C). When two cyclic esters with comparable reactivity are mixed together in a C-IROP system, a block copolymer can be produced by sequential addition to this living system [57]. Last, but not least, ROP of lactones can also proceed through free radical polymerization [58]. This method is a powerful tool for enabling the introduction of various functional groups into the polymer by chain growth rather than step growth. By free radical polymerization, it is conceivable to design polymers with similar or inferior density than the monomers. This displays a remarkable importance for applications where it is required to keep a constant volume throughout the polymerization such as tooth fillings, coatings, and others [59].

1.5 Potential

It is envisioned that bicyclic terpenoids, with the additional fused ring system shown in red (Figure 1), could be upgraded to novel terpene-based materials. Monoterpenes and their lactone derivatives exhibited a great interest due to their valuable characteristics. Lactone derivatives can be polymerized and used in value-added applications, this includes biodegradable composites of plastics [60], drug delivery vectors, and scaffolds in tissue engineering [61]. Lactone polymers are appropriate biomedical starting materials for copolymerization and blending to design

medical devices with fascinating mechanical properties and degradation kinetics.

Norcamphor (**19**) is a ketone ($C_7H_{10}O$) readily available through synthesis [62] and with a structure closely related to that of bicyclic terpenes (Figure 1). In this part, we will shed some light on the chemical conversion of norcamphor (**19**) into its lactone derivatives (**20** and **21**) via Baeyer–Villiger (BV) reaction, and the feasibility to polymerize these lactones through ROP using methanesulfonic acid (MSA) as a catalyst. BV oxidation was reported as an efficient reaction to convert cyclohexanones to lactones [63, 64]. Likewise, BV oxidation of **19** has been reported [65]. The oxidation of **19** by BV using *m*-CPBA as an oxidizing agent can result in the formation of **20** and **21** lactones (Scheme S2). The characteristics and the chemical structures of the lactones were investigated by nuclear magnetic resonance (NMR) analysis (^{1}H, ^{13}C, COSY, and HSQC NMR). By ^{1}H NMR, we were able to estimate the conversion (%) of **19** into its lactone derivatives (Figure S1). It is indicated that the conversion of **19** into either **20** or **21** is 100%, as evidenced by the total disappearance of proton $H_{a'}$ (2.68 ppm) after BV reaction. H_a is shifted down-field to H_a (4.88 ppm) in case of **20**; however, in the case of **21**, $H_{e'1}$ (2.05 ppm) and $H_{e'2}$ (1.86 ppm) of **19** were also shifted down-field to $H_{\varepsilon 1}$ (4.33 ppm) and $H_{\varepsilon 2}$ (4.12 ppm), respectively. Furthermore, based on the ^{1}H NMR data, the chemical BV oxidation of **19** resulted in the formation of **20** (93.4%) and a trace amount of **21** (6.6%).

The products were separated by column chromatography and we were able to retain 96.1% pure **20** lactone form (Figure S2). The spectral data (^{1}H and HSQC) confirmed that the retained lactone is **20** (Figure S2). The value of chemical shift of H_a (single proton) in the ^{1}H NMR spectra of **20** is 4.88 ppm, which reveals that this proton is attached to a carbon linked with an alkoxy oxygen atom. This provides a clear indication that the oxygen atom is inserted between carbon C_a and the carbonyl functionality.

Furthermore, the enzymatic transformation of **19** into the normal lactone **20** was performed with the *Escherichia coli* cell lysate containing the cyclohexanone monooxygenase from *Acinetobacter calcoaceticus* ($CHMO_{Acineto}$) containing amino acid variations for increased stability ($CHMO_{Acineto}$–QM) [43]. The *E. coli* cell lysate containing $CHMO_{Acineto}$–QM was also analyzed in terms of activity on nicotinamide adenine dinucleotide phosphate (NADPH), using both the natural substrate cyclohexanone and norcamphor **19**, which showed a volumetric activity of 1.318 ± 0.049 U mL^{-1} and 1.088 ± 0.090 U mL^{-1}, respectively. These data corroborate the high activity of the biocatalyst toward **19** (assuming similar uncoupling for the two substrates), in line with previous reports [65]. The high industrial potential of applying oxidoreductases in biosynthesis at larger scale has been discussed recently [37]. The biotransformation in the presence of FAD, cofactor regeneration system containing glucose dehydrogenase (GDH) and glucose, with NADPH and catalase for the uncoupling reaction, allowed 100% conversion of **19** into **20**, with a 100% presence of the normal lactone under our working conditions. The results were analyzed by GC/FID analysis (Figure S5). The upscale of the reaction was performed in a 2 L baffled flask containing 200 mL of the reaction described above. After 24 h, 100% conversion was identified by GC/FID, responding to 50 mg product formed. To sum up, our results showed an extraordinary chemo-selective BV oxidation of 96% and 100% toward the formation of the isomer **20**, using chemical and enzymatic catalysis, respectively. In the case of chemical transformation, it is attributed to the mechanism of action of BV reaction as discussed by Corma et al. [66].

1.6 Polymerization of lactone 20

Herein, we report the polymerization of lactone **20** using the ROP method through a cationic mechanism as shown in Scheme 1B. Benzyl alcohol (BnOH) was used as an initiator and MSA as a highly efficient catalyst for the ROP of lactones [67]. We have recently shown that this catalysts is suitable to generate novel biopolymers by ROP from bicyclic terpene-derived lactones [54]. The polymerization of **20** is illustrated in Scheme 2. Figure 2 shows the crude ^{1}H NMR spectra of polymer **20** after 24 h of reaction. Herein, we were able to confirm the polymerization of **20** for the first time, as the proton H_{am} at 4.88 ppm (H_a in the monomeric form lactone) is shifted down-field to H_{ap} (H_a after polymerization) at 5.18 ppm. The polymer conversion (PC%) representing the percentage of lactone **20** monomer that undergoes polymerization, and the degree of polymerization (DP) representing the number average length of lactone **20**, indicated a PC of 75.23% and an average DP of 19.2. Based on the average DP, the molecular weight (*M*n) of the synthesized polymer was estimated to be 2.23×10^3 g mol^{-1}.

The molecular weight was further assessed by size exclusion chromatography (SEC) (Figure 3). In agreement

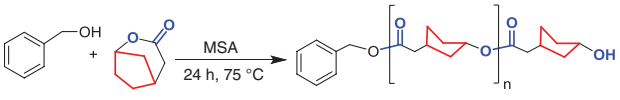

Scheme 2: Illustration of ROP of lactone **20** using BnOH as an initiator and MSA as a catalyst.

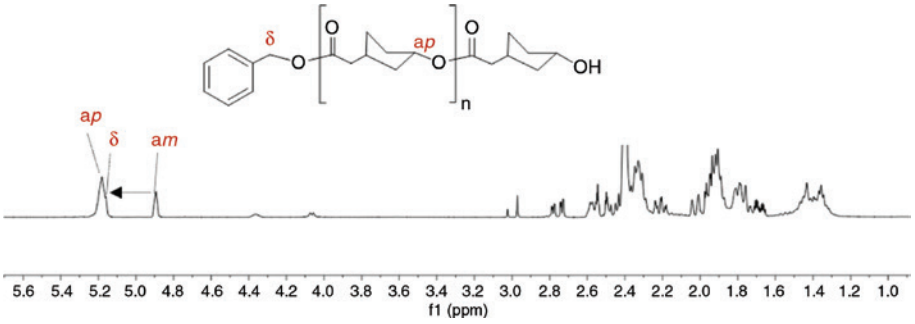

Figure 2: ^{1}H NMR spectra of lactone **20** polymer (crude) after 24 h of reaction.

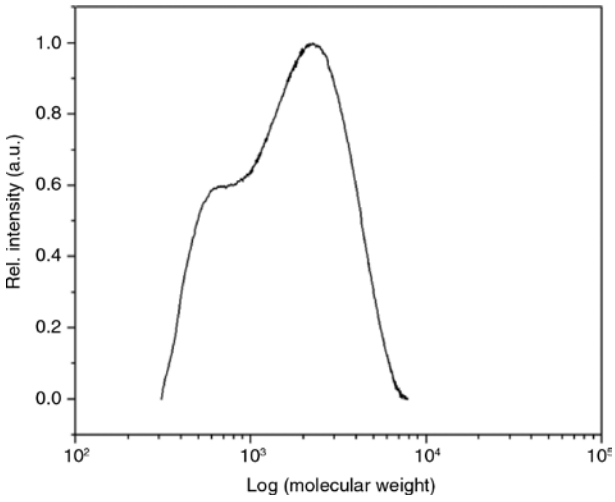

Figure 3: Size exclusion chromatography of lactone **20** polymer (crude) after 24 h of reaction.

with the NMR results, SEC data showed that the produced polymer has the following molecular weight: *M*n 1.38×10^{3} g mol^{-1} and *M*w 2.16×10^{3} g mol^{-1} with an intermediate polydispersity of *Đ* 1.56. The SEC results showed a minor difference from the NMR data. In fact, molecular weight measured by SEC was confounded because SEC was most sensitive to the hydrodynamic volume of the polymer; ROP added weight to the molecule but did not necessarily increase the hydrodynamic volume in proportion to the increase in the length of the polymer. Our data in combination revealed that ROP is an efficient method to polymerize bicyclic terpene-based lactones, which could serve as green substituents to other aliphatic polyesters.

2 Conclusions

Norcamphor, which represented a bicyclic terpene model system, was oxidized into the corresponding lactone using chemical and enzymatic methods. Both methods showed high efficiency and chemo-selectivity toward the formation of the normal lactone. The chemically synthesized lactone was further polymerized using CROP. The resulting unprecedented polyester had a molecular weight of 1.4 kg/mol and a polydispersity of 1.56. Although the polymerization was not performed in large scale or under fully inert conditions, our results show the potential of upgrading natural building blocks into novel materials. It is worth noticing that this newly explored polymer, and most probably other unexplored terpene-derived polymers, will have the potential to augment the replacement of synthetic materials with bio-based alternatives in novel sustainable applications. We anticipate that oxidoreductases will enable the generation of key monomeric building blocks even at a larger scale, which would fully unlock the potential of a biocatalytic toolbox in the generation of terpene-based materials.

3 Experimental

3.1 Materials

Norcamphor 98% (CAS 497-38-1) was provided by Sigma-Aldrich (St. Louis, MO, USA). Kanamycin sulfate, Isopropyl β-D-1-thiogalactopyranoside, nicotinamide adenine dinucleotide phosphate, and flavine adenine dinucleotide were purchased from Sigma-Aldrich (St. Louis, MO, USA). Methanesulfonic acid (MSA, CAS 75-75-2) was provided by Sigma-Aldrich (St. Louis, MO, USA). Benzyl alcohol anhydrous, 99.8% (CAS 100-51-6) from Sigma-Aldrich (St. Louis, MO, USA). NMR spectra were recorded using Bruker Avance III 400 MHz spectrometer (Bruker, Billerica, MA, USA). SEC is performed using A TOSOH EcoSEC HLC-8320GPC system (Tokyo, Japan) equipped with an EcoSEC RI detector and three PSS PFG 5 µm columns (microguard, 100 Å, and 300 Å). The GC/FID and GC/MS analysis were performed on a GCMS-QP2010 Ultra (Shimadzu, Kyoto, Japan) equipped with an AOC-20i autoinjector (Shimadzu,

Kyoto, Japan). Rxi-5ms capillary columns (30 m × 250 μm × 0.25 μm, Restek, Bellefonte, PA, USA).

3.2 Bacterial strain, plasmids, and media

The in-house available gene of the BVMO (cyclohexanone monooxygenase) from *A. calcoaceticus*, previously cloned in the plasmid pET28a(+) vector containing an N-terminal His_6-tag, was transformed into *E. coli* BL21(DE3) for expression. The cells were grown in 2×YT medium (16 g L^{-1} tryptone, 10 g L^{-1} yeast extract, 5 g L^{-1} sodium chloride) containing 40 μg mL^{-1} kanamycin sulfate (Sigma, St. Louis, MO, USA). Cell density at OD_{600} was determined using a plate reader SpectraMax i3x (Molecular Devices, San José, CA, USA).

3.3 Recombinant expression and preparation of cell lysate

Freshly transformed *E. coli* BL21(DE3) cells were inoculated in 1 mL 2× YT medium containing 40 μg mL^{-1} kanamycin sulfate in 96-deep well plates, and were cultivated overnight at 37 °C and 200 rpm. The overnight culture was used to inoculate 3 mL of fresh medium to $OD_{600} = 0.1$ and incubated at 37 °C and 200 rpm until an $OD_{600} = 0.6–0.8$ was reached. Induction was carried out for 20 h at 25 °C and 180 rpm using 0.05 mM isopropyl β-D-1-thiogalactopyranoside (IPTG) (Sigma-Aldrich, USA). Cells were harvested by centrifugation at 2276 × *g* for 15 min at 4 °C on a Thermo Scientific Sorvall ST16R centrifuge coupled to a M20 rotor (Waltham, MA, USA). Cell lysis was performed with B-PER Complete Bacterial Protein Extraction Reagent (Thermo Fisher Scientific, Waltham, MA, USA) using 5 mL g^{-1} to resuspend the cell pellet. The solution was incubated at room temperature for 15 min under mixing (750 rpm) to lyse the cells. The cell debris were removed by centrifugation at 2276×*g* for 30 min at 4 °C.

For high-scale conversion, a preculture of 30 mL 2× YT medium containing 40 μ g mL^{-1} kanamycin sulfate was incubated overnight at 37 °C and 200 rpm. The overnight culture was diluted in 200 mL of fresh medium to $OD_{600} = 0.1$ and incubated at 37 °C and 200 rpm until an $OD_{600} = 0.6–0.8$ was reached. Induction and cell harvesting were performed as described above. Tris-buffer pH 8.5 and 50 mM (5 mL) was used to resuspend the wet cell pellet (1 g). The suspension was sonicated for 1 min with 1 s pulse and 2 s pause (total time 3 min), 60% duty cycle under ice cooling with Misonix sonifier cell disruptor ultrasonic S-4000 probe (MIsonix Inc., Farmingdale, NY, USA). Cellular debris were removed by centrifugation at 40,000×*g* and 4 °C for 20 min.

3.4 Protein analysis

The protein concentration was measured by Bradford using the Bio-Rad protein assay kit (Bio-Rad, Hercules, CA, USA) with bovine serum albumin as the protein standard. Sodium dodecyl sulfate-polyacrylamide gel electrophoresis was performed according to Laemmli [68], using a 4% stacking and 15% separating gels, purchased from Bio-Rad. SeeBlue Plus2 prestained protein standard was purchased from Thermo Fisher Scientific and used as a molecular weight marker. Proteins were stained using InstantBlue (Expedeon, Heidelberg, Germany) .

3.5 BVMO activity by NADPH measurements

The measurement of the activity of the *E. coli* cell lysate containing $CHMO_{Acineto}$—QM was performed spectrophotometrically, using the Spark TECAN plate reader (Männedorf, Switzerland). A total of 20 μL of cell lysate was mixed with 200 μL reaction mixture (50 mM Tris-HCl pH 8.5, 0.6 mM cyclohexanone or norcamphor (60 mM in ethanol), 0.25 mM NADPH. The consumption of reduced NADPH was determined at 340 nm for 120 s in 96-well plates (using an extinction coefficient of $\varepsilon_{NADPH} = 6.4\ mM^{-1}\ cm^{-1}$).

3.5.1 Biocatalytic lactone synthesis

Biocatalysis reactions were carried out with cell lysate in 96-deep well plates sealed with a breathable seal, at 30 °C and 200 rpm for 24 h. The cell lysate (40 μL) was mixed with 0.2 mM (NADPH, from a 0.1 M stock in 50 mM Tris-HCl pH 8.5) and 2 mM norcamphor (1 M stock in ethanol), supplemented with 62 μM FAD (62 mM stock in 50 mM Tris-HCl pH 8.5) and 290 U mL^{-1} of catalase from bovine liver. The GDH cofactor regeneration system was used adding GDH (Codexis, Redwood City, CA, USA) at a concentration of 0.09 mg mL^{-1} and activity 0.03 U μL^{-1} with 0.2 M D-glucose (1 M stock in 50 mM Tris-HCl, pH 8.5).

Scale-up conversions were performed in 2-L baffled shake flasks to increase oxygen supply to the reaction. The flasks contained a reaction volume of 200 mL and were sealed with a breathable seal. The cell lysate (16 mL) was added to the reaction as described above. The reaction was carried out at 30 °C and 200 rpm.

3.5.2 Extraction of biocatalysis samples and GC analysis

Biocatalysis reactions were extracted twice with 500 µL ethyl acetate spiked with 2 mM decane as internal standard. Each extraction was followed by vortexing for 5 s and centrifugation at 9000× *g* for 10 min. The organic phase was analyzed by GC/FID and GC/MS on a GCMS-QP2010 Ultra (Shimadzu, Japan) equipped with an AOC-20i autoinjector (Shimadzu, Japan). Rxi-5ms capillary columns (30 m × 250 µm × 0.25 µm, Restek, USA) were used with argon as the carrier gas. A Sky Liner PTV 2010 liner with glass wool was used as an inlet liner and a splitless injection mode (1 µL) was used with the following GC temperatures: injection port, 225 °C; initial column temperature, 50 °C; first temperature ramp, 10 °C min^{-1}; second column temperature, 150 °C; second temperature ramp, 20 °C min^{-1}; third temperature, 300 °C; third temperature ramp, 3 °C min^{-1}; fourth temperature, 340 °C; final hold time, 10 min; total run time 30.83 min. The MSD source was kept at 200 °C, interface temperature at 200 °C. The solvent was delayed for 2 min.

3.6 Chemical synthesis of lactones

A total of 4.06 g of 77% pure *m*-CPBA was dissolved in dichloromethane (DCM), dried over magnesium sulfate, filtered, and then concentrated under nitrogen flow. Once the *m*-CPBA (18.13 mmol, 2 eq) is pure, 1.8 mL of DCM and 1 g of norcamphor (0.9 mmol, 1 eq) were added to a three-neck flask to obtain a final concentration of 0.5 M. The reaction was stirred under reflux for 18 h at room temperature under nitrogen atmosphere. The organics were washed twice with sodium bisulfite and twice with sodium bicarbonate to remove excess of *m*-CPBA, and then dried over magnesium sulfate. The product was then purified on column using (10% EtOAc in heptane over 2CV then up to 30% EtOAc in heptane over 8CV). DCM was dried over aluminum oxide before use. Final yield was 53.2% with 532 mg of lactone recovered.

3.7 Polymerization of lactone 20

The ROP method was used to polymerize lactone **20**. Briefly, 128 mg of lactone **20** (1.02 mmol, 1 eq), 1.06 µL of benzyl alcohol (0.01 eq), and 1.32 µL of MSA (0.02 eq) were poured into a 2 mL vial containing 0.5 mL toluene and mixed at 75 °C under nitrogen flow. The reaction was stopped after 24 h and MSA activity was quenched by adding 1.8 µL pyridine. The crude specimens were used for analysis.

PC (%) and DP were estimated by ^{1}H NMR based on the peak intensity of the corresponding signals according to the following equation:

$$\text{PC}\,(\%) = \frac{\text{Lactone } \mathbf{20}\,(\text{polymerized})}{\text{Lactone } \mathbf{20}\,(\text{total})} \times 100$$

$$= \frac{I(\text{Ha}_p)}{I(\text{Ha}_p + \text{Ha}_m)} \times 100$$

$$\text{DP} = \frac{\text{Lactone } \mathbf{20}\,(\text{polymerized})}{\text{BnOH}\,(\text{terminal})} = \frac{2 \times I(\text{Ha}_p)}{I(\text{H}\delta)}$$

where (*I*) is the integral (area) of the selected proton and Hδ are the two protons of the carbon linked to alkoxy oxygen atom in BnOH after polymerization.

3.8 Nuclear magnetic resonance

NMR spectra (^{1}H, ^{13}C, homonuclear correlation spectroscopy (^{1}H-^{1}H COSY), and heteronuclear single-quantum correlation (HSQC)) were recorded using Bruker Avance III 400 MHz spectrometer (Billerica, MA, USA), equipped with a 5 mm multinuclear broad band probe (BBFO+) and *z*-gradient coil. The samples (~20 mg) were dissolved in d_1-chloroform (~1 mL) and the spectra were recorded at room temperature and with 16 scans for 1D ^{1}H, 256 scans for 1D ^{13}C, and 2 scans for 2D ^{1}H-^{1}H COSY and 2D ^{1}H-^{13}C HSQC. Chemical shifts (in ppm) were expressed relative to the resonance of chloroform ($\delta = 7.26$ ppm).

3.9 Size exclusion chromatography

The molecular weight of the synthesized lactone **20**-based polymer was determined by SEC analysis. A TOSOH EcoSEC HLC-8320GPC system (Minato City, Tokyo, Japan) was used equipped with an EcoSEC RI detector and three PSS PFG 5 µm columns (microguard, 100 Å, and 300 Å). Polyethylene glycol standards were used for calibration, and toluene was used as internal standard. DMF was used to dissolve **20** crude.

Acknowledgments: This work was generously funded by a FORMAS young research leader grant (#942-2016-66). The PDC Center for High Performance Computing at the Royal Institute of Technology (KTH) is greatly acknowledged.

References

1. Oldfield E, Lin F-Y. Terpene biosynthesis: modularity rules. Angew Chem Int Ed Engl 2012;51:1124–37.
2. Zi J, Mafu S, Peters RJ. To gibberellins and beyond! Surveying the evolution of (di)terpenoid metabolism. Annu Rev Plant Biol 2014;65:259–86.
3. Kato N, Comer E, Sakata-Kato T, Sharma A, Sharma M, Maetani M, et al. Diversity-oriented synthesis yields novel multistage antimalarial inhibitors. Nature 2016;538:344–9.
4. Thimmappa R, Geisler K, Louveau T, O'Maille P, Osbourn A. Triterpene biosynthesis in plants. Annu Rev Plant Biol 2014;65:225–57.
5. Surendra K, Corey EJ. Highly enantioselective proton-initiated polycyclization of polyenes. J Am Chem Soc 2012;134:11992–4.
6. Schalk M, Pastore L, Mirata MA, Khim S, Schouwey M, Deguerry F, et al. Toward a biosynthetic route to sclareol and amber odorants. J Am Chem Soc 2012;134:18900–3.
7. Zhuang X, Chappell J. Building terpene production platforms in yeast. Biotechnol Bioeng 2015;112:1854–64.
8. Krieg T, Sydow A, Faust S, Huth I, Holtmann D. CO_2 to terpenes: autotrophic and electroautotrophic α-humulene production with cupriavidus necator. Angew Chem Int Ed 2018;57:1879–82.
9. Rabe P, Rinkel J, Nubbemeyer B, Köllner TG, Chen F, Dickschat JS. Terpene cyclases from social amoebae. Angew Chem Int Ed 2016;55:15420–3.
10. Guenther A, Hewitt CN, Erickson D, Fall R, Geron C, Graedel T, et al. A global model of natural volatile organic compound emissions. J Geophys Res Atmos 1995;100:8873–92.
11. Sindelarova K, Granier C, Bouarar I, Guenther A, Tilmes S, Stavrakou T, et al. Global data set of biogenic VOC emissions calculated by the MEGAN model over the last 30 years. Atmos Chem Phys 2014;14:9317–41.
12. Zhu Y, Romain C, Williams CK. Sustainable polymers from renewable resources. Nature 2016;540:354–62.
13. Winnacker M. Pinenes: abundant and renewable building blocks for a variety of sustainable polymers. Angew Chem Int Ed 2018;57:14362–71.
14. Snyder SA, Tang Z-Y, Gupta R. Enantioselective total synthesis of (–)-napyradiomycin A1 via asymmetric chlorination of an isolated olefin. J Am Chem Soc 2009;131:5744–5.
15. Eriksson A, Kürten C, Syrén PO. Protonation-initiated cyclization by a class II terpene cyclase assisted by tunneling. ChemBioChem 2017;18:2301–5.
16. Ren F, Feng X, Ko TP, Huang CH, Hu Y, Chan HC, et al. Insights into TIM-barrel prenyl transferase mechanisms: crystal structures of PcrB from *Bacillus subtilis* and *Staphylococcus aureus*. ChemBioChem 2013;14:195–9.
17. Wong CP, Awakawa T, Nakashima Y, Mori T, Zhu Q, Liu X, et al. Two distinct substrate binding modes for the normal and reverse prenylation of hapalindoles by the prenyltransferase AmbP3. Angew Chem Int Ed 2018;57:560–3.
18. Itoh T, Tokunaga K, Radhakrishnan EK, Fujii I, Abe I, Ebizuka Y, et al. Identification of a key prenyltransferase involved in biosynthesis of the most abundant fungal meroterpenoids derived from 3,5-dimethylorsellinic acid. ChemBioChem 2012;13:1132–5.
19. Awakawa T, Mori T, Nakashima Y, Zhai R, Wong CP, Hillwig ML, et al. Molecular insight into the Mg^{2+} – dependent allosteric control of indole prenylation by aromatic prenyltransferase AmbP1. Angew Chem Int Ed 2018;57:6810–3.
20. Elshahawi SI, Cao H, Shaaban KA, Ponomareva LV, Subramanian T, Farman ML, et al. Structure and specificity of a permissive bacterial C-prenyltransferase. Nat Chem Biol 2017;13:366–8.
21. Zhang L, Chen C-C, Ko T-P, Huang J-W, Zheng Y, Liu W, et al. Moenomycin biosynthesis: structure and mechanism of action of the prenyltransferase MoeN5. Angew Chem Int Ed 2016;55:4716–20.
22. Chen RD, Gao BQ, Liu X, Ruan FY, Zhang Y, Lou JZ, et al. Molecular insights into the enzyme promiscuity of an aromatic prenyltransferase. Nat Chem Biol 2017;13:226–34.
23. Christianson DW. Structural and chemical biology of terpenoid cyclases. Chem Rev 2017;117:11570–648.
24. Ruzicka L. The isoprene rule and the biogenesis of terpenic compounds. Experientia 1953;9:357–67.
25. Köksal M, Chou WK, Cane DE, Christianson DW. Structure of geranyl diphosphate *C*-methyltransferase from *Streptomyces coelicolor* and implications for the mechanism of isoprenoid modification. Biochemistry. 2012;51:3003–10.
26. Eichhorn E, Locher E, Guillemer S, Wahler D, Fourage L, Schilling B. Biocatalytic process for (–)-ambrox production using squalene hopene cyclase. Adv Synth Catal 2018;360:2339–51.
27. Seitz M, Syrén PO, Steiner L, Klebensberger J, Nestl BM, Hauer B. Synthesis of heterocyclic terpenoids by promiscuous squalene-hopene cyclases. ChemBioChem 2013;14:436–9.
28. Hammer SC, Marjanovic A, Dominicus JM, Nestl BM, Hauer B. Squalene hopene cyclases are protonases for stereoselective Brønsted acid catalysis. Nat Chem Biol 2015;11:121–6.
29. Ignea C, Pontini M, Motawia MS, Maffei ME, Makris AM, Kampranis SC. Synthesis of 11-carbon terpenoids in yeast using protein and metabolic engineering. Nat Chem Biol 2018;14:1090–8.
30. Kühnel LC, Nestl BM, Hauer B. Enzymatic Addition of Alcohols to Terpenes by Squalene Hopene Cyclase Variants. ChemBioChem 2017;18:2222–5.
31. Roth S, Funk I, Hofer M, Sieber V. Chemoenzymatic synthesis of a novel borneol-based polyester. ChemSusChem 2017;10:3574–80.
32. Miyaji H, Satoh K, Kamigaito M. Bio-based polyketones by selective ring-opening radical polymerization of α-pinene-derived pinocarvone. Angew Chem Int Ed 2016;55:1372–6.
33. Hernandez-Ortega A, Vinaixa M, Zebec Z, Takano E, Scrutton NS. A toolbox for diverse oxyfunctionalisation of monoterpenes. Sci Rep 2018;8:14396.
34. Seifert A, Antonovici M, Hauer B, Pleiss J. An efficient route to selective bio-oxidation catalysts: an iterative approach comprising modeling, diversification, and screening, based on CYP102A1. ChemBioChem 2011;12:1346–51.
35. Bell SG, Chen X, Sowden RJ, Xu F, Williams JN, Wong LL, et al. Molecular recognition in (+)-alpha-pinene oxidation by cytochrome P450cam. J Am Chem Soc 2003;125:705–14.
36. Wang Y, Lan D, Durrani R, Hollmann F. Peroxygenases en route to becoming dream catalysts. What are the opportunities and challenges? Curr Opin Chem Biol 2017;37:1–9.
37. Dong J, Fernández-Fueyo E, Hollmann F, Paul CE, Pesic M, Schmidt S, et al. Biocatalytic oxidation reactions: a chemist's perspective. Angew Chem Int Ed 2018;57:9238–61.
38. Nealon CM, Musa MM, Patel JM, Phillips RS. Controlling substrate specificity and stereospecificity of alcohol dehydrogenases. ACS Catal 2015;5:2100–14.
39. Oberleitner N, Peters C, Rudroff F, Bornscheuer UT, Mihovilovic MD. *In vitro* characterization of an enzymatic redox cascade composed of an alcohol dehydrogenase, an enoate reduc-

tases and a Baeyer–Villiger monooxygenase. J Biotechnol 2014;192:393–9.
40. Stuermer R, Hauer B, Hall M, Faber K. Asymmetric bioreduction of activated C=C bonds using enoate reductases from the old yellow enzyme family. Curr Opin Chem Biol 2007;11:203–13.
41. Oberleitner N, Ressmann AK, Bica K, Gärtner P, Fraaije MW, Bornscheuer UT, et al. From waste to value – direct utilization of limonene from orange peel in a biocatalytic cascade reaction towards chiral carvolactone. Green Chem 2017;19:367–71.
42. Lygidakis A, Karuppiah V, Hoeven R, Ní Cheallaigh A, Leys D, Gardiner JM, et al. Pinpointing a mechanistic switch between ketoreduction and "ene" reduction in short-chain dehydrogenases/reductases. Angew Chem Int Ed 2016;55:9596–600.
43. Balke K, Beier A, Bornscheuer UT. Hot spots for the protein engineering of Baeyer-Villiger monooxygenases. Biotechnol Adv 2018;36:247–63.
44. Morrill C, Jensen C, Just-Baringo X, Grogan G, Turner NJ, Procter DJ. Biocatalytic conversion of cyclic ketones bearing α-quaternary stereocenters into lactones in an enantioselective radical approach to medium-sized carbocycles. Angew Chem Int Ed 2018;57:3692–6.
45. Oberleitner N, Peters C, Muschiol J, Kadow M, Saß S, Bayer T, et al. An enzymatic toolbox for cascade reactions: a showcase for an in vivo redox sequence in asymmetric synthesis. ChemCatChem 2013;5:3524–8.
46. Morita M, Hao Y, Jokela JK, Sardar D, Lin Z, Sivonen K, et al. Post-translational tyrosine geranylation in cyanobactin biosynthesis. J Am Chem Soc 2018;140:6044–8.
47. Carter-Franklin JN, Butler A. Vanadium bromoperoxidase-catalyzed biosynthesis of halogenated marine natural products. J Am Chem Soc 2004;126:15060–6.
48. Butler A, Sandy M. Mechanistic considerations of halogenating enzymes. Nature 2009;460:848.
49. Gally C, Nestl BM, Hauer B. Engineering rieske non-heme iron oxygenases for the asymmetric dihydroxylation of alkenes. Angew Chem Int Ed 2015;54:12952–6.
50. Hauenstein O, Agarwal S, Greiner A. Bio-based polycarbonate as synthetic toolbox. Nat Commun 2016;7:11862.
51. Messiha HL, Ahmed ST, Karuppiah V, Suardíaz R, Ascue Avalos GA, Fey N, et al. Biocatalytic routes to lactone monomers for polymer production. Biochemistry 2018;57:1997–2008.
52. Lowe JR, Martello MT, Tolman WB, Hillmyer MA. Functional biorenewable polyesters from carvone-derived lactones. Polym Chem 2011;2:702–8.
53. Shin J, Lee Y, Tolman WB, Hillmyer MA. Thermoplastic elastomers derived from menthide and tulipalin A. Biomacromolecules 2012;13:3833–40.
54. Stamm A, Biundo A, Schmidt B, Brücher J, Lundmark S, Olsén P, et al. ChemBioChem 2019 (in revision). DOI: cbic.201900046.
55. Albertsson AC, Varma IK. Recent developments in ring opening polymerization of lactones for biomedical applications. Biomacromolecules 2003;4:1466–86.
56. Brode GL, Koleske JV. Lactone polymerization and polymer properties. J Macromol Sci 1972;6:1109–44.
57. Stridsberg KM, Ryner M, Albertsson A-C. Controlled ring-opening polymerization: polymers with designed macromolecular architecture. In: Degradable aliphatic polyesters. Berlin, Heidelberg: Springer, 2002:41–65.
58. Phelan M, Aldabbagh F, Zetterlund PB, Yamada B. Mechanism and kinetics of the free radical ring-opening polymerization of cyclic allylic sulfide lactones. Polymer 2005;46:12046–56.
59. Nuyken O, Pask SD. Ring-opening polymerization – an introductory review. Polymers 2013;5:361–403.
60. Jaakkola T, Rich J, Tirri T, Närhi T, Jokinen M, Seppälä J, et al. In vitro Ca-P precipitation on biodegradable thermoplastic composite of poly(epsilon-caprolactone-co-DL-lactide) and bioactive glass (S53P4). Biomaterials 2004;25:575–81.
61. Farhat W, Venditti R, Ayoub A, Prochazka F, Fernández-de-Alba C, Mignard N, et al. Towards thermoplastic hemicellulose: Chemistry and characteristics of poly-(ε-caprolactone) grafting onto hemicellulose backbones. Mater Des 2018;153:298–307.
62. Kleinfelter DC, Schleyer PvR. 2-Norbornanone. Org Synth 1962;42:79–82.
63. ten Brink GJ, Arends IW, Sheldon RA. The Baeyer-Villiger reaction: new developments toward greener procedures. Chem Rev 2004;104:4105–24.
64. Ratus B, Gladkowski W, Wawrzenczyk C. Lactones 32: New aspects of the application of Fusarium strains to production of alkylsubstituted ε-lactones. Enzyme Microb Technol 2009;45:156–63.
65. Gagnon R, Grogan G, Levitt MS, Roberts SM, Wan PWH, Willetts AJ. J Chem Soc Perkin 1 1994;2537–43.
66. Corma A, Nemeth LT, Renz M, Valencia S. Sn-zeolite beta as a heterogeneous chemoselective catalyst for Baeyer-Villiger oxidations. Nature 2001;412:423–5.
67. Dove AP. Organic catalysis for ring-opening polymerization. ACS Macro Lett 2012;1:1409–12.
68. Laemmli UK. Cleavage of structural proteins during the assembly of the head of bacteriophage T4. Nature 1970;227:680–5.

Supplementary Material: The online version of this article offers supplementary material (https://doi.org/10.1515/znc-2018-0199).